7410 J. Med. Chem. 2009, 52, 7410–7420
DOI: 10.1021/jm900461w

Journal of Medicinal Chemistry Article

Synthesis and in Vitro Evaluation of N-Substituted Maleimide Derivatives as Selective Monoglyceride Lipase Inhibitors

Nicolas Matuszak, Giulio G. Muccioli,† Geoffray Labar, and Didier M. Lambert*

Endocannabinoid and Cannabinoid Research Group, Drug Design and Discovery Centre, Unité de Chimie Pharmaceutique et de Radiopharmacie, Louvain Drug Research Institute, Ecole de Pharmacie, Faculté de Médecine, Université Catholique de Louvain, 73 Avenue E. Mounier UCL-CMFA (7340), B-1200 Bruxelles, Belgium. †Present address: Bioanalysis and Pharmacology of Bioactive Lipids Laboratory, Louvain Drug Research Institute, Université Catholique de Louvain, 72 Avenue E. Mounier UCL-CHAM (7230), B-1200 Bruxelles, Belgium.

Received April 10, 2009

The endocannabinoid 2-arachidonoylglycerol (2-AG) plays a major role in many physiological processes, and its action is quickly terminated via enzymatic hydrolysis catalyzed by monoglyceride lipase (MGL). Regulating its endogenous level could offer therapeutic opportunities; however, few selective MGL inhibitors have been described so far. Here, we describe the synthesis of N-substituted maleimides and their pharmacological evaluation on the recombinant human fatty acid amide hydrolase (FAAH) and on the purified human MGL. A few *N*-arylmaleimides were previously described (Saario, S. M.; Salo, O. M.; Nevalainen, T.; Poso, A.; Laitinen, J. T.; Jarvinen, T.; Niemi, R. Characterization of the Sulfhydryl-Sensitive Site in the Enzyme Responsible for Hydrolysis of 2-Arachidonoylglycerol in Rat Cerebellar Membranes. *Chem. Biol.* 2005, *12*, 649−656) as MGL inhibitors, and along these lines, we present a new set of maleimide derivatives that showed low micromolar IC_{50} and high selectivity toward MGL vs FAAH. Then, structure−activity relationships have been investigated and, for instance, 1-biphenyl-4-ylmethylmaleimide inhibits MGL with an IC_{50} value of 790 nM. Furthermore, rapid dilution experiments reveal that these compounds act as irreversible inhibitors. In conclusion, N-substituted maleimides constitute a promising class of potent and selective MGL inhibitors.

Introduction

Modulating the level of the endocannabinoids anandamide and 2-arachidonoylglycerol (2-AG[a]) through their biosynthesis or degradation pathways can constitute a therapeutic approach for numerous pathological states, including multiple sclerosis, pain and inflammation, and different types of cancer.[2] To date, four enzymes responsible for the inactivation of endocannabinoids via their hydrolysis have been characterized at the molecular level: fatty acid amide hydrolase (FAAH),[3] monoglyceride lipase (MGL),[4,5] a recently discovered type-2 FAAH,[6] *N*-acylethanolamine hydrolyzing acid amidase (NAAA).[7] Moreover, two serine hydrolases, namely, ABHD6 and ABHD12, have been proposed by Blankman et al.[8] as new 2-AG hydrolyzing enzymes in mouse brain.

MGL is a 33 kDa serine hydrolase hydrolyzing the 2- or 1 (3)-ester bond of monoglycerides to fatty acids and glycerol.[9] MGL hydrolyzes one of the major endocannabinoids, 2-AG, an endogenous full agonist at CB_1 and CB_2 cannabinoid receptors,[10,11] which is known to act as a retrograde messenger.[12] MGL has been purified, and its cDNA was isolated and cloned from adipose tissue.[4,5] This protein, containing two lipase motives (active serine motif GXSXG and the HG dipeptide) with a Ser122/His269/Asp239 catalytic triad (evidenced by mutagenesis studies[4]), is predicted to belong to the α/β hydrolase fold family and is found abundant in brain tissue, particularly at presynaptic terminals[13] and in areas of the brain where CB_1 cannabinoid receptors are also localized. The relevance of MGL to 2-AG metabolism has been shown by Dinh et al. who demonstrated that overexpression of MGL in rat neurons reduced the accumulation of 2-AG[14] and that RNA interference-mediated silencing of MGL expression enhanced 2-AG accumulation in HeLa cells.[15] However, they showed that half of the 2-AG hydrolyzing activity remains detectable after MGL was immunodepleted from cytosolic brain fractions, suggesting that other metabolic pathways are involved in 2-AG degradation.[15] More recently, Muccioli and co-workers discovered a 2-AG hydrolase activity in microglial cells[16] distinct from that of MGL which could be assigned to ABDH6.[17] This underlines the need of new efficient pharmacological tools such as purified enzymes or selective and efficient MGL inhibitors. Furthermore, as the sequence homology between murine and human proteins is only 83%,[18] the use of a human enzyme can provide relevant information about the enzyme and will minimize the differences in drug−enzyme interactions between in vitro and in vivo effects in human.

*To whom correspondence should be addressed. Phone: +32-2-764-7347. Fax: +32-2-764-7363. E-mail: didier.lambert@uclouvain.be.

[a] Abbreviations: 2-AG, 2-arachidonoylglycerol; ATFMK, arachidonyltrifluoromethylketone; BSA, bovine serum albumin; CB, cannabinoid; DEAD, diethylazodicarboxylate; FAAH, fatty acid amide hydrolase; MAFP, methylarachidonyl fluorophosphonate; MGL, monoglyceride lipase; NAAA, *N*-acylethanolamine-hydrolyzing acid amidase; NAM, *N*-arachidonylmaleimide; 2-OG, 2-oleoylglycerol; Ph, phenyl; PPh_3, triphenylphosphine; THF, tetrahydrofuran.

 Published on Web 07/07/2009

Table 1. Structures of Previously Reported MGL Inhibitors[b]

Abbreviation	Structures	hMGL IC_{50} (nM)	hFAAH IC_{50} (nM)	selectivity ratio
NAM	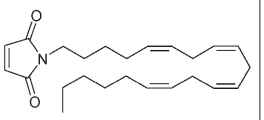 **1**	1120 ± 140	2180 ± 620	1.95
MAFP	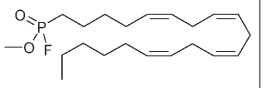	26.30 ± 9.95	0.33 ± 0.07	0.01
ATFMK	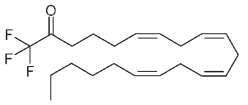	6310 ± 730	12.3 ± 1.13	0.002
URB602	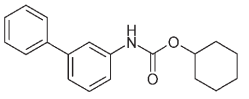	10 000 ± 2565	5650 ± 690	0.57
LY2183240	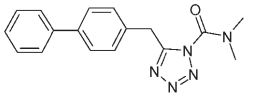	54.4 ± 5.2	37.3 ± 5.4	0.68
JZL184	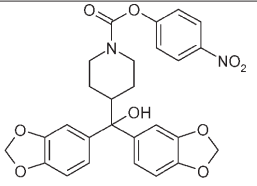	6[a]	4000[a]	667[a]

[a] Values were from the original publication of Long[21] from mouse recombinant enzymes. No SEM was provided in the reference. [b] Determination of their selectivity profile of known MGL inhibitors on hMGL versus hFAAH. Values are expressed as mean ± SEM from three independent experiments performed in duplicate.

From a medicinal chemistry point of view, few MGL inhibitors are available and they often lack selectivity or have not been evaluated on both human MGL and human FAAH.[19,20] A recent breakthrough has been done with the report of 4-nitrophenyl 4-(dibenzo[*d*][1,3]dioxol-5-yl-(hydroxy)methyl)piperidine-1-carboxylate (JZL184)[21] as a potent and selective MGL inhibitor. The administration of this MGL inhibitor clearly demonstrated that a selective blockade of 2-arachidonoylglycerol hydrolysis, without modifying anandamide levels in the brain, produces cannabinoid behavioral effects. Apart from this compound, MGL can be inhibited by various nonspecific serine hydrolase inhibitors, such as methylarachidonyl fluorophosphonate (MAFP), hexadecylsulfonyl fluoride, and phenylmethylsulfonyl fluoride.[9,22] On the basis of MGL sensitivity to free sulfhydryl group-modifying agents such as *p*-chloromercuribenzoate and mercury chloride, Saario and co-workers[1] investigated the sensitivity of MGL to maleimide derivatives, well-known Michael acceptors. Among them, *N*-arachidonylmaleimide (NAM, **1**) with a reported IC_{50} value of 140 nM was the most active in the series. Although **1** was not the most potent MGL inhibitor, it exhibits a promising selectivity profile. As a preliminary experiment, the inhibitory potential of human-MGL vs human-FAAH has been measured for five different MGL inhibitors (Table 1) **1**, MAFP, arachidonyltrifluoromethylketone

Scheme 1. Synthesis of the *N*-Phenylmaleimides (**2**−**28**), *N*-Alkylphenylmaleimides (**29**−**36**), *N*-Phenylsuccinimide (**37**), *N*-Phenylphtalimide (**38**), 3-Methylphenylmaleimide (**39**), 3,4-Dimethylphenylmaleimide (**40**), and 1,3-Diphenylmaleimide (**41**)[a]

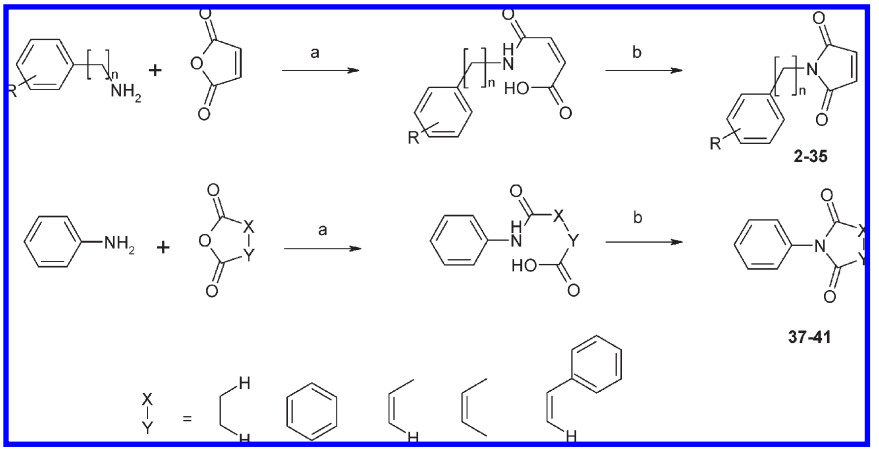

[a] Reagents and conditions: (a) stirred in diethyl ether for 1 h and filtered off; (b) then stirred in acetic anhydride with sodium acetate (0.5 equiv) for 30 min on a steam bath.

Scheme 2. Synthesis of *N*-Alkylmaleimides (**44**−**46**)[a]

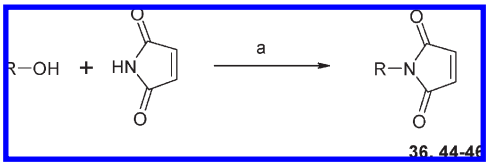

[a] Reagents and conditions: (a) $Pd(PPh_3)_4$ (1 equiv), neopentyl alcohol (0.5 equiv), DEAD (1 equiv) stirred overnight in THF.

(ATFMK), biphenyl-3-ylcarbamic acid cyclohexyl ester (URB602), 5-biphenyl-4-ylmethyltetrazole-1-carboxylic acid dimethylamide (LY2183240). On the basis of the observation that **1** and *N*-phenylmaleimide (**2**) both appeared to be good MGL inhibitors[1] with a high selectivity profile, we report here the synthesis of a series of *N*-phenylmaleimides, *N*-alkylmaleimides, and bismaleimides and their pharmacological characterization on both human recombinant FAAH and MGL. We describe the structure−activity relationships among these three subfamilies of maleimides and their selectivity profile toward MGL, with respect to some of the few known MGL inhibitors. Their mechanism of inhibition has also been investigated.

Results

Chemistry. The N-substituted maleimides described herein were synthesized following two main routes. The first one (Scheme 1, method A[23]) involves a substituted aniline or an aliphatic amine and maleic anhydride as building blocks, whereas the second one requires a primary alcohol and maleimide (Scheme 2, method B[24]). The *N*-phenylmaleimides (**2**−**35**) were readily obtained using method A by reacting the desired substituted aniline with maleic anhydride in diethyl ether, leading to the corresponding *N*-phenylmaleanic acid, which precipitates in diethyl ether. Without any further purification, this open intermediate was subsequently cyclized in acetic anhydride in the presence of sodium acetate to the *N*-phenylmaleimide of interest (**2**−**35**). 1-Biphenyl-4-ylmethylmaleimide (**36**) and the *N*-alkylmaleimide derivatives (**44**−**46**) were obtained using the Mitsunobu procedure (method B). Therefore, the relevant alkyl alcohol was stirred with maleimide in the presence of neopentyl alcohol, triphenylphosphine (PPh_3), and diethylazodicarboxylate (DEAD) in anhydrous tetrahydrofuran (THF), as outlined in Scheme 2.

N-Phenylsuccinimide (**37**) and *N*-phenylphtalimide (**38**) were obtained following method A, starting from succinic anhydride and phthalic anhydride, respectively. Using the same method but starting from citraconic anhydride, 2,3-dimethylmaleic anhydride, and 2-phenylmaleic anhydride gave 3-methyl-1-phenylmaleimide (**39**), 3,4-dimethyl-1-phenylmaleimide (**40**), and 1,3-diphenylmaleimide (**41**), respectively. The bismaleimide derivative (**49**) was synthesized using 1,4-benzenedimethanamine and maleic anhydride (method A).

Structure−Activity Relationships. As a first step, we wanted to test the hypothesis stating that **2** inhibits MGL through a nucleophilic attack on its olefinic double bond. Indeed, Saario et al. showed that the succinimide analogues of the active maleimide were devoid of any activity against MGL.[1] However, those data were obtained on a tissue preparation rather than using a pure MGL preparation, and therefore, the substrate hydrolysis seen by Saario and colleagues could have been at least partially the result of a 2-oleoylglycerol hydrolysis through a non-MGL activity. Thus, we decided either to remove the double bond of the maleimide moiety such in **37** or to render it unreactive with respect to a Michael addition such as for phenylphthalimide **38**. Both compounds were unable to inhibit MGL, even when tested at millimolar concentrations (Table 2). We also tested if increasing the steric hindrance around the double bond (**39**−**41**) would be as detrimental to the activity as removing it. Indeed the double bond of compounds **39**−**41** is less accessible to the enzyme nucleophilic attack, resulting in a reduction of about half of MGL activity when tested at 1 mM.

Taken together, these data confirm that the presence of a freely accessible double bond is a key parameter to MGL inhibition by maleimide derivatives. Since the double bond is essential to the inhibition, the maleimide motif was kept unchanged and the effect of the N-substitution on the inhibitory potency was explored (Table 3). Three series of compounds, *N*-phenylmaleimides (**2**−**35**), *N*-alkylmaleimides (**42**−**46**), and bismaleimides (**47**−**53**), were evaluated on purified human MGL activity.

Table 2. Structures and Inhibition Potential of *N*-Phenylmaleimide, *N*-Phenylsuccinimide, *N*-Phenylphtalimide, and Hindered Double-Bond Maleimides toward hMGL and hFAAH Activity[a]

compound	structure	hMGL IC_{50} (μM)	hFAAH IC_{50} (μM)
2	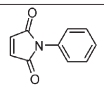	15.9 ± 2.8	229 ± 28
37	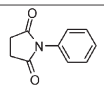	0% at 1 mM	0% at 1 mM
38	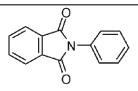	0% at 1 mM	0% at 1 mM
39	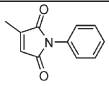	50% at 1 mM	0% at 1 mM
40	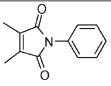	57% at 1 mM	206 ± 36
41	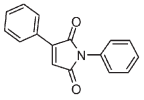	50% at 1 mM	0% at 1 mM

[a] Values are expressed as mean ± SEM from three independent experiments performed in duplicate for the IC_{50} values. In the absence of IC_{50} values, percentages of inhibition at 1 mM are given.

In order to study the importance of the alkyl chain length and position on the phenyl ring, a series of alkyl-substituted *N*-phenylmaleimides (i.e., *N*-(alkylphenyl)maleimides, **2**−**12**) was synthesized. The *N*-(alkylphenyl)maleimides showed MGL inhibition properties with IC_{50} values ranging from 2.00 to 14.10 μM. The best inhibition was observed with compounds bearing a methyl or an ethyl group in position 2. In order to investigate the influence of a longer alkyl chain linked to the phenyl ring, we also tested *N*-(4-heptylphenyl)-maleimide **12**. Only small differences in the MGL inhibitory activity were observed when the side chain in position 4 of the phenyl ring was lengthened from two (**8**, IC_{50} = 2.82 μM) to seven carbons (**12**, IC_{50} = 2.12 μM). On the contrary, if the side chain in position 4 is shortened to one carbon (**5**, IC_{50} = 14.10 μM) or is replaced by H (**2**, IC_{50} = 15.9 μM), the inhibitory activity is significantly reduced. Note that these *N*-(alkylphenyl)maleimides showed a good selectivity profile for MGL toward FAAH, with IC_{50} values on FAAH ranging from 65 μM to values above 500 μM (Table 3).

We next synthesized compounds with more hydrophilic substituents, such as hydroxy or alkoxy substituents (**13**−**16**), on the phenyl ring. *N*-(4-Hydroxyphenyl)maleimide (**13**, IC_{50} = 12.9 μM) had a similar potency compared with **2**, whereas the alkoxy-substituted compounds (**14**−**16**) showed inhibition values ranging between 5.75 μM (**16**) and 6.92 μM (**14**). These two series of compounds retained the same selectivity factor of 100−300 for MGL compared to FAAH.

The following step in this series was to investigate the effect of halogen substitution on the phenyl ring. Twelve *N*-(halogenophenyl)maleimide derivatives varying by the nature and position of the halogen atom were synthesized (**17**−**28**). These compounds showed inhibition activity, with IC_{50} values ranging from 2.24 to 7.24 μM, the best inhibition being obtained with *N*-(3-iodophenyl)maleimide (**27**, IC_{50} = 2.24 μM). Upon analysis of the data reported in Table 3, it is apparent that the size of the halogen has little influence on the inhibition; indeed, regardless of the position, there was no significant difference between the fluorine-substituted compounds (**17**−**19**) and the iodine-substituted compounds (**26**−**28**). For instance, *N*-(4-fluorophenyl)maleimide (**19**, IC_{50} = 5.18 μM), *N*-(4-chlorophenyl)maleimide (**22**, IC_{50} = 7.24 μM), *N*-(4-bromophenyl)maleimide (**25**, IC_{50} = 4.37 μM), and *N*-(4-iodophenyl)maleimide (**28**, IC_{50} = 4.34 μM) all showed a similar inhibitory potency toward MGL. However, the position of the substituent had some influence on the inhibition potential; as for all the halogens, position 3 was preferred to positions 2 and 4. A possible explanation could be that the attractive inductive effect of the halogens in position 3 lowers the electronic density of the double bond which in turn makes it more sensitive to a nucleophilic attack. Moreover, this series still showed good selectivity toward MGL, with most IC_{50} values for FAAH inhibition being above 200 μM.

The next step in the structure−activity relationships studies reported here consisted of adding a phenyl ring to the *N*-phenylmaleimide moiety, resulting in three *N*-biphenylmaleimide derivatives (**29**−**31**, Table 4). When compared to **2** (IC_{50} = 15.90 μM), there was a 10-fold increase in MGL inhibition with IC_{50} values around 2 μM for **29**−**31**. Note that, as previously observed, the position of the phenyl substituent had no influence on MGL inhibition. As the electronic effect of the phenyl substituent cannot explain here the evolution of the inhibitory potential, it seems that the steric effect of the biphenyl moiety or a π−π interaction with an aromatic residue in the active site of MGL could play a role in the enhancement of inhibition. Contrary to what is observed for MGL, the phenyl substituent position has a great influence on the inhibition of FAAH activity, with 1-biphenyl-4-ylmaleimide (**31**, IC_{50} = 5.89 μM) being 30 times more active than 1-biphenyl-2-ylmaleimide (**29**, IC_{50} = 180 μM).

Interestingly, introducing a methylene spacer between the maleimide and the 4-biphenyl motif led to a further increase of MGL inhibition, as observed with **36** (IC_{50} = 0.79 μM).

Because the presence of a methylene spacer increased MGL inhibition, we investigated the influence of the spacer arm between the maleimide moiety and the phenyl ring. Thus, we synthesized three derivatives characterized by a spacer of increasing length between the maleimide and the phenyl moieties (**32**−**34**, Table 4). All three compounds, 1-benzylmaleimide (**32**), 1-phenethylmaleimide (**33**), and 1-(4-phenylbutyl)maleimide (**34**), proved to be more potent compared to **2**.

The compounds gained in activity when the phenyl or biphenyl moiety is spaced out from the maleimide ring; the IC_{50} value is 3−7 times lower when the phenyl ring is spaced out from the maleimide backbone (compound **2** vs **32**−**34**) and is also 2 times better when there is a methylene between the maleimide ring and the biphenyl moiety (compound **31** vs **36**). Finally, as seen with the other series, all these compounds retained selectivity for MGL vs FAAH.

Our second major series of N-substituted maleimides was the *N*-alkylmaleimides (Table 5). Indeed, *N*-ethylmaleimide (**43**) was shown to inhibit the hydrolysis of 2-AG in rat cerebellar membranes with an IC_{50} value of 53 μM.[1] In our hands, by the use of a purified human recombinant MGL, **43** inhibited 2-OG hydrolysis with an IC_{50} value of 16.6 μM. The shorter analogue, *N*-methylmaleimide (**42**), was slightly

Table 3. hMGL and hFAAH Inhibition by *N*-Phenylmaleimide Derivatives **3**−**28**[a]

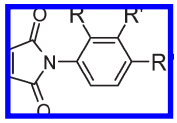

compd	R	R′	R″	IC$_{50}$ (μM) hMGL	IC$_{50}$ (μM) hFAAH	selectivity
3	CH_3	H	H	2.69 ± 0.33	> 500	> 200
4	H	CH_3	H	2.75 ± 0.48	> 500	> 200
5	H	H	CH_3	14.10 ± 1.70	> 500	> 150
6	CH_2CH_3	H	H	2.00 ± 143	> 500	> 150
7	H	CH_2CH_3	H	4.68 ± 0.57	103 ± 7	22
8	H	H	CH_2CH_3	2.82 ± 0.27	163 ± 12	58
9	H	H	$(CH_2)_2CH_3$	5.89 ± 0.57	186 ± 65	32
10	$CH(CH_3)_2$	H	H	7.86 ± 0.95	65 ± 10	9
11	H	H	$CH(CH_3)_2$	2.88 ± 0.43	120 ± 18	40
12	H	H	$(CH_2)_6CH_3$	2.12 ± 0.35	87 ± 18	41
13	H	H	OH	12.90 ± 2.2	288 ± 50	30
14	OCH_3	H	H	6.92 ± 0.84	> 500	78
15	H	OCH_3	H	6.60 ± 0.47	> 500	> 200
16	H	H	OCH_3	5.75 ± 0.56	> 500	> 200
17	F	H	H	4.47 ± 0.55	295 ± 50	63
18	H	F	H	2.39 ± 0.35	89 ± 16	37
19	H	H	F	5.18 ± 0.45	120 ± 21	23
20	Cl	H	H	4.17 ± 0.51	214 ± 88	77
21	H	Cl	H	2.82 ± 0.20	102 ± 26	39
22	H	H	Cl	7.24 ± 1.10	112 ± 11	7
23	Br	H	H	2.92 ± 0.52	> 500	75
24	H	Br	H	4.27 ± 0.31	151 ± 58	27
25	H	H	Br	4.37 ± 0.53	51 ± 12	50
26	I	H	H	5.01 ± 0.36	200 ± 124	37
27	H	I	H	2.24 ± 0.22	62 ± 11	45
28	H	H	I	4.34 ± 0.80	60 ± 4	14

[a] Values are expressed as the mean ± SEM from three independent experiments performed in duplicate.

Table 4. Inhibition Values of *N*-Biphenylmaleimides (**29**−**31**), *N*-Alkylphenylmaleimides (**32**−**34**), 1-(4-Ethylbenzyl)maleimide (**35**), and 1-Biphenyl-4-ylmethylmaleimide (**36**) on hMGL and hFAAH Activity[a]

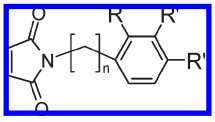

compd	*n*	R	R′	R″	IC$_{50}$ (μM) hMGL	IC$_{50}$ (μM) hFAAH	selectivity
29	0	Ph	H	H	1.55 ± 0.23	180 ± 57	116
30	0	H	Ph	H	2.34 ± 0.29	49 ± 6.0	21
31	0	H	H	Ph	1.62 ± 0.16	5.89 ± 2.0	4
32	1	H	H	H	5.14 ± 0.76	186 ± 38	36
33	2	H	H	H	7.61 ± 1.13	249 ± 79	33
34	4	H	H	H	2.14 ± 0.49	85 ± 13	39
35	1	H	H	ethyl	3.55 ± 0.53	123 ± 12	35
36	1	H	H	Ph	0.79 ± 0.23	16.6 ± 3.8	73

[a] Values are expressed as the mean ± SEM from three independent experiments performed in duplicate.

Table 5. Inhibition Values of *N*-Methylmaleimide (**42**), *N*-Ethylmaleimide (**43**), and *N*-Alkylmaleimides (**44**−**46**) on hMGL and hFAAH[a]

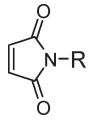

compd	R	IC$_{50}$ (μM) hMGL	IC$_{50}$ (μM) hFAAH	selectivity
1	arachidonyl	1.12 ± 0.14	2.18 ± 0.62	1.95
42	methyl	24.5 ± 3.0	40% at 1 mM	
43	ethyl	16.6 ± 1.6	35% at 1 mM	
44	nonyl	3.55 ± 0.43	40.7 ± 8.2	12
45	hexadecyl	2.69 ± 1.38	0% at 1 mM	
46	oleyl	0.93 ± 0.16	26% at 1 mM	

[a] values are expressed as mean ± SEM from 3 independent experiments performed in duplicate for the IC$_{50}$ values, in absence of IC$_{50}$ values, percentages of inhibition at 1 mM are given).

less active (IC$_{50}$ = 24.5 μM). As might be expected, a longer substituent such as the one of *N*-nonylmaleimide (**44**) resulted in an increased inhibition of MGL (**46**, IC$_{50}$ = 3.55 μM). Note that the activity was only slightly modified by a further increase of the alkyl chain length as observed with *N*-hexadecylmaleimide (**45**, IC$_{50}$ = 2.69 μM). Interestingly, the closest substrate analogues (i.e., *N*-oleylmaleimide (**46**) and **1**) were only slightly more active, with IC$_{50}$ values of 0.93 and 1.12 μM, respectively, even if we can postulate that the introduction of a double bond in the alkyl chain allows a better interaction with MGL. Thus, compared to the nonyl derivative, the increase of the alkyl chain length results in less soluble derivatives without significant gain in activity. These compounds retained selectivity toward MGL inhibition, with FAAH inhibition IC$_{50}$ values in the millimolar range. Note that the somewhat lower activity for **1** compared to what was first reported by

Saario et al.[1] is in line with what we previously reported[25,26] and to what Blankman et al. found using rat brain membranes.[8]

Saario et al.[1] suggested the presence of two cysteine residues (Cys 208 and Cys 242) in the vicinity of MGL active site that would explain the activity of the maleimide derivatives. Thus, we hypothesized that a compound bearing two reactive moieties (i.e., two maleimides) could be more prone to potently inhibit MGL. This hypothesis was investigated by testing a series of bismaleimides derivatives varying by the nature of their linker (Scheme 3 and Table 6).

Two close analogues of **2**, phenyl-1,3-bismaleimide (**47**) and phenyl-1,4-bismaleimide (**48**), were first assayed against MGL. As illustrated in Table 5, **47** demonstrated low micromolar inhibition value toward MGL. However, no significant difference was observed between the 1,3- and the 1,4- analogues. These compounds are 8 times more potent on MGL than **2**. We next increased the flexibility of the linker by synthesizing compounds **49** and **50**, which inhibited MGL with IC_{50} values of 1.70 and 2.24 μM, respectively. Finally, compounds with an even more flexible linker (i.e., butyl (**51**), hexyl (**52**), and bis-1,2-diethoxyethane (**53**)) were assayed without noting any further increase of the activity (IC_{50} values of 28.8, 1.70, and 1.95 μM, respectively). When **50** (IC_{50} = 1.70 μM) was compared with its analogue lacking the second maleimide moiety (**35**, IC_{50} = 3.55 μM), it appears that a second maleimide moiety does not result in an increased inhibitory potency. Furthermore, **51** and **52** showed IC_{50} values of the same magnitude as their corresponding *N*-alkylmaleimides analogues. This suggests that either reacting with one residue is sufficient to fully inhibit the enzyme or that the two potentially reactive cysteine residues are not close enough to allow a single molecule to react with both of them.

Table 6. Structures and Inhibitory Activities of the Bismaleimides Assayed in This Study[a] Regarding hMGL and hFAAH

	IC_{50} (μM)		
compd	hMGL	hFAAH	selectivity
47	2.03 ± 0.30	37.2 ± 11.8	18
48	2.22 ± 0.45	13.49 ± 2.90	6
49	1.70 ± 0.21	16.6 ± 2.90	10
50	2.24 ± 0.30	10.7 ± 1.03	5
51	28.8 ± 6.60	8.32 ± 2.65	0.3
52	1.70 ± 0.16	18.2 ± 2.69	11
53	1.95 ± 0.34	80% at 1 mM	

[a] IC_{50} values or percent of inhibition at 1 mM. In the absence of IC_{50} values, percentages of inhibition at 1 mM are given.

As these compounds are assumed to act via a Michael addition on the cysteine residues of the enzyme, preincubation of the enzyme with maleimide inhibitors would facilitate and enhance the covalent addition, thus increasing the inhibitory potential of such compounds. As a first approach, we investigated the influence of different preincubation times on the inhibitory potency of *N*-phenylmaleimide **2** and1, 4-bis-(malimido)xylene **49** (Figure 1). These compounds showed higher inhibition values following 15 and 30 min of preincubation with the enzyme. The most relevant effect of preincubation was noticed after 30 min, demonstrating that the inhibitory effect of such compounds could be enhanced by preincubating them with the enzyme.

Then, we investigated whether these compounds act as reversible or irreversible MGL inhibitors. MAFP and ATFMK were used as controls for an irreversible and reversible MGL inhibition, respectively.[26−28] We tested **1** and two of our best MGL inhibitors so far: **36** and **49** (Figure 2).

After rapid dilution, MAFP, known as irreversible inhibitor, still inhibited 83% of MGL activity while ATFMK, reported as reversible one, only inhibited 26% of MGL

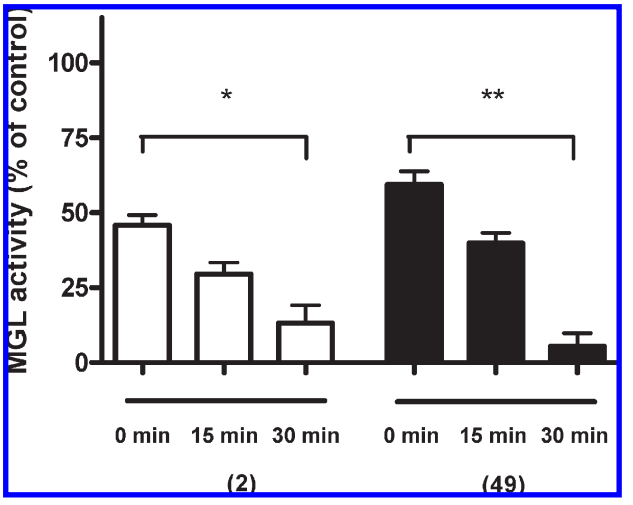

Figure 1. Influence of the preincubation of **2** and **49** on the inhibition of the purified human MGL activity.
N-Phenylmaleimide (**2**) and 1,4-bis(malimido)xylene (**49**) were preincubated at their IC_{50} value for 0, 15, and 30 min with human purified MGL. Data shown are the mean of three experiments performed in duplicate. Statistical significance was assessed by one-way ANOVA followed by a Dunett post-test (∗, $P < 0.05$; ∗∗, $P < 0.01$) relative to no-preincubated samples.

Scheme 3. Structure of the Bismaleimides Used in This Study

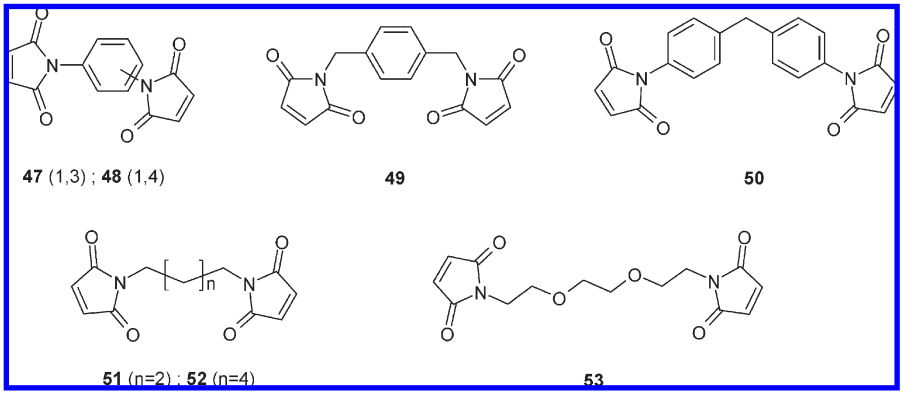

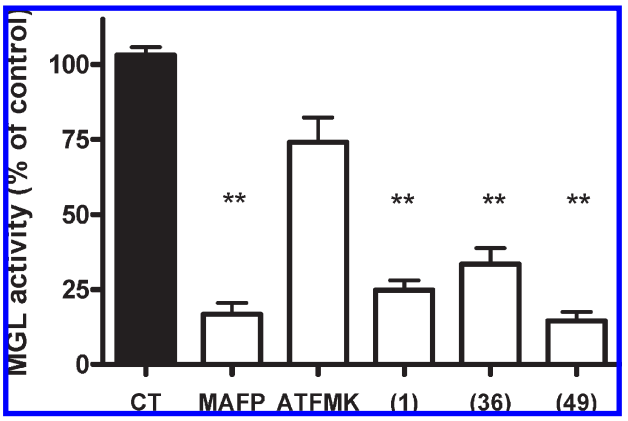

Figure 2. Irreversible inhibition assay of several MGL inhibitors (MAFP, ATFMK, **1**, **36**, **49**) with purified human MGL.
All compounds were assayed at 40 times their IC_{50} value except ATFMK at 20 times its IC_{50} value on human purified MGL. Dimethyl sulfoxide was taken as a control. Data shown are the mean of three experiments performed in duplicate. Statistical significance was assessed by one-way ANOVA followed by a Dunett post-test (∗, $P < 0.05$; ∗∗, $P < 0.01$), relative to DMSO.

activity. All three maleimides tested showed similar behavior compared with the one observed with MAFP, thus still inhibiting from 69% to 86% of MGL activity after a 400-fold dilution into assay buffer. As expected, these results taken together validated the hypothesis that these compounds act as covalent inhibitors of MGL and that the inhibitory potential of such inhibitors is enhanced by a preincubation with the enzyme.

Conclusion

Here, we report the synthesis and structure−activity relationship studies of maleimide-type MGL inhibitors. The maleimide family could present many advantages. First, used as probes, they could give new interesting data about the enzyme's environment, as they react with particular amino acids. Indeed, recently, using mass spectrometry and mutational analysis, Zvonok and co-workers[28,29] gave new information about the recombinant enzyme catalytic site using **1**, confirming Saario's first hypothesis and pushing us forward to use our inhibitors as "informers" about the local environment of the enzyme. Second, as Michael acceptors, they are good irreversible inhibitors, and thus, the role of MGL in 2-AG degradation could be efficiently evaluated. Indeed, Burston et al. demonstrated that **1** could reveal the in vitro activity of 2-AG and enhance the effects of 2-AG through inhibition of MGL.[30] However, this class of agents also presents some limitations. Indeed, their high reactivity with free thiols may cause them to cross-react with other proteins that depend on cysteine residues for their function.

From a therapeutic point of view, the design of endocannabinoid hydrolases inhibitors may be a chance for the treatment of several pathological states such as inflammatory pain[31] or anxiety. Indeed, the elevation of the endocannabinoid levels directly where endocannabinoids are produced and needed would allow for higher selectivity compared to the systemic use of cannabinoid agonists.

The inhibitors presented here demonstrated good inhibition toward MGL with IC_{50} values in the low micromolar range for most of them. Besides their relative potency, it is important to note that these inhibitors are quite selective when compared to their FAAH activity. It seems determinant for the enzyme inhibition that the maleimide moiety is substituted by a large lipophilic group (biphenyl) and spaced out from the maleimide ring: indeed, the best inhibitor of our series is **36**, with an IC_{50} value of 790 nM on MGL and a selectivity index of 73 toward FAAH. Previously described MGL inhibitors have been assessed for their potency in stress induced analgesia[32] or their antinociceptive effects,[31,33,34] and compounds like **36** or **46** could produce the same beneficial effects. Furthermore, the maleimide derivatives' mechanism of inhibition is comparable to that of **1**, which was recently shown to enhance 2-AG effects in vivo.[29] In comparison to the high lipophilicity of **1** (clogP value of 6.12) and of **46** (clogP value of 6.12), compound **36** exhibited a higher inhibitory potential as well as a reduced lipophilicity (clogP value of 2.89). This could represent a new horizon in the treatment of diseases where the imbalance of endocannabinoids has been proved to play a major role, like in CNS diseases and in the treatment of pain and psychiatric disorders (depression, anxiety, etc.).

Experimental Section

Chemistry. All reagents were purchased from commercial sources (Sigma-Aldrich or Acros) and were used without further purification. Solvents were of analytical grade. Bismaleimidobutane (1-(4-(2,5-dioxo-2*H*-pyrrol-1(5*H*)-yl)butyl)-1*H*-maleimide) (**51**), bismaleimidohexane (1-(6-(2,5-dioxo-2*H*-pyrrol-1(5*H*)-yl)-hexyl)-1*H*-maleimide) (**52**), and 1,8-bis-maleimidodiethyleneglycol (**53**) were bought from Thermo Fisher Scientific, and 1,1′-(methylenedi-4,1-phenylene)bismaleimide (**50**) was purchased from Acros Organics. *N*,*N*′-(1,3-phenylene)dimaleimide (**47**), *N*,*N*′-(1,4-phenylene)dimaleimide (**48**), *N*-methylmaleimide (**42**), and *N*-ethylmaleimide (**43**) were from Sigma-Aldrich, and *N*-arachidonylmaleimide (**1**) was bought from Cayman Chemicals. Nuclear magnetic resonance (^{1}H NMR, ^{13}C NMR) spectra were recorded at room temperature on a Bruker Avance 400 operating at 400 MHz for ^{1}H and 100 MHz for ^{13}C. Chemical shifts (δ) are reported relative to the tetramethylsilane peak set at 0.00 ppm. In the case of multiplets, the signals are reported as intervals. Signals were abbreviated as s, singlet; d, doublet; t, triplet; q, quadruplet; m, multiplet. Melting points (mp) were determined in open capillaries using an Electrothermal 9100 apparatus and are reported uncorrected. Mass spectra were recorded on a Finningan MAT 44S, with an ionization voltage of 70 eV.

All tested compounds were at least 95% pure on the basis of HPLC−MS using a LTQ Orbitrap mass spectrometer (ThermoFisher Scientifc) coupled to an Accela HPLC system (ThermoFisher Scientific). Separation was achieved using a Luna LC-18 column (5 μM, 4.60 mm × 250 mm) (from Phenomenex).

Elemental analyses were performed for original compounds on a Carlo Erba EA 1108 analyzer (Carlo Erba, Milano, Italy) and are within ±0.4% of the theoretical values; values are presented in the Supporting Information. Liquid film infrared (IR) spectra were recorded using a Perkin-Elmer FT-IR 286 spectrometer, and values are reported as λ in cm^{-1}; relevant peaks are presented in the Supporting Information.

General Procedures. 3-Phenylaniline (30a). 30a was obtained through a Suzuki coupling. Briefly, to a stirred solution of 3-bromoaniline (2.2 mL, 20 mmol) in toluene (100 mL) were added $Pd(PPh_3)_4$ (0.924 g, 0.80 mmol), a solution of Na_2CO_3 (16.59 g, 20 mmol) in H_2O (50 mL), and a solution of phenylboronic acid (4.98 g, 40 mmol) in EtOH (50 mL) under N_2 atmosphere. The mixture was vigorously stirred under reflux overnight. Once the mixture cooled, water was added, and the mixture was extracted with CH_2Cl_2. The combined organic layers were dried (Na_2SO_4) and concentrated under reduced pressure. Purification of the residue by silica column

chromatography (hexane/EtOAc 1:4) gave 3-phenylaniline as a yellow solid (3.26 g, 96%). GC−MS m/z 170 (MH^+). ^{1}H NMR ($CDCl_3$) δ 6.67 (d, 1H), 6.90 (s, 1H), 6.99 (d, 1H), 7.22 (t, 1H), 7.32 (t, 1H), 7.55 (d, 2H), 7.40 (t, 2H). ^{13}C NMR ($CDCl_3$) δ 114.0, 114.2, 117.8, 127.1, 127.2, 128.6, 129.7, 141.4, 142.5, 146.6.

General Procedure for the Preparation of *N*-Arylmaleimides (Method A) (Compounds 2−36). In a 100 mL three-necked flask provided with a stirrer, a reflux condenser, and a dropping funnel were placed 1.96 g (20 mmol) of maleic anhydride (or succinic anhydride) and 25 mL of diethyl ether. The maleic anhydride dissolved upon stirring, at which point a solution of 1 equiv (20 mmol) of the appropriate aniline in 5 mL of diethyl ether was run through the dropping funnel. The resulting thick suspension was stirred at room temperature for 1 h and was then cooled in an ice bath. The N-substituted maleanic acid was recovered by filtration and dried and subsequently added to a flask containing a solution of anhydrous sodium acetate (0.65 g, 8 mmol) in acetic anhydride (6.7 mL) and stirred over a steam bath for 30 min. The reaction mixture was then cooled to room temperature in a cold water bath and was then poured into 100 mL of an ice−water mixture. The precipitated product was recovered by filtration, washed three times with 30 mL portions of ice-cold water, and dried. The crude N-substituted maleimide was recrystallized from ethanol/water to afford the desired product.

1-(2-Methylphenyl)maleimide (3). Beige crystalline solid. Yield: 84%. Mp 47−48 °C. GC−MS m/z 188 (MH^+). ^{1}H NMR ($CDCl_3$) δ 2.12 (s, 3H), 6.73 (s, 2H), 7.08 (s, 1H), 7.23−7.30 (m, 3H). ^{13}C NMR ($CDCl_3$) δ 17.8, 126.8, 128.7, 129.3, 130.1, 131.0, 131.0, 134.2, 136.9, 169.6.

1-(3-Methylphenyl)maleimide (4). Yellow crystalline solid. Yield: 78%. Mp 35−38 °C. GC−MS m/z 188 (MH^+). ^{1}H NMR (DMSO-d_6) δ 3.36 (t, 1H), 7.21 (s, 1H), 7.17 (s, 2H), 7.12 (d, 2H). ^{13}C NMR ($CDCl_3$) δ 21.0, 123.0, 126.5, 128.5, 128.6, 130.7, 133.8, 138.9, 169.3.

1-(4-Methylphenyl)maleimide (5). Yellow powder. Yield: 91%. Mp 158−160 °C. GC−MS m/z 188 (MH^+). ^{1}H NMR (DMSO-d_6) δ 2.38 (s, 3H), 6.82 (s, 2H), 7.20 (d, 2H), 7.26 (d, 2H). ^{13}C NMR ($CDCl_3$) δ 21.1, 126.0, 128.5, 129.8, 134.2, 138.1, 169.7.

1-(2-Ethylphenyl)maleimide (6). White crystalline solid. Yield: 73%. Mp 60−61 °C. GC−MS m/z 202 (MH^+). ^{1}H NMR ($CDCl_3$) δ 1.13 (t, 3H), 2.44 (q, 2H), 7.06 (d, 1H), 7.26 (t, 1H), 7.34−7.39 (m, 2H). ^{13}C NMR ($CDCl_3$) δ 14.2, 24.3, 126.8, 129.0, 129.3, 129.5,129.7, 134.3, 142.4, 170.0.

1-(3-Ethylphenyl)maleimide (7). Yellow crystalline solid. Yield: 68%. Mp 80−82 °C. GC−MS m/z 202 (MH^+). ^{1}H NMR (DMSO-d_6) δ 1.19 (t, 3H), 3.64 (q, 2H), 7.14 (t, 2H), 7.17 (s, 2H), 7.25 (d, 1H), 7.39 (t, 1H). ^{13}C NMR (DMSO-d_6) δ 15.0, 27.5, 123.8, 125.8, 126.9, 128.4, 131.2, 134.3, 144.2, 169.6.

1-(4-Ethylphenyl)maleimide (8). Golden solid. Yield: 89%. Mp 65−68 °C. GC−MS m/z 202 (MH^+). ^{1}H NMR ($CDCl_3$) δ 1.24 (t, 3H), 2.65 (q, 2H), 6.81 (d, 2H), 7.21−7.28 (m, 2H). ^{13}C NMR ($CDCl_3$) δ 15.5, 28.6, 100.1, 126.2, 128.7, 128.8, 128.9, 134.3, 144.4, 169.8.

1-(4-Propylphenyl)maleimide (9). Golden solid. Yield: 44%. Mp < 30 °C. GC−MS m/z 216 (MH^+). ^{1}H NMR ($CDCl_3$) δ 1.50 (t, 3H), 2.57 (m, 2H), 3.42 (t, 2H), 7.00 (s, 2H), 7.17 (d, 2H), 7.26 (t, 2H). ^{13}C NMR (DMSO-d_6) δ 27.5, 28.1, 34.5, 36.8, 125.6, 128.2, 134.4, 141.8, 171.0.

1-(2-Isopropylphenyl)maleimide (10). Yellow crystalline solid. Yield: 79%. Mp 114−116 °C. GC−MS m/z 216 (MH^+). ^{1}H NMR ($CDCl_3$) 1.57 (s, 6H), 4.04 (s, 2H), 6.86 (s, 2H), 6.88−6.91 (m, 2H), 7.27 (d, 1H), 7.60 (d, 1H). ^{13}C NMR ($CDCl_3$) δ 30.9, 121.5, 127.4, 130.3, 132.3, 134.3, 169.1.

1-(4-Isopropylphenyl)maleimide (11). Yellow crystalline solid. Yield: 55%. Mp 70−72 °C. GC−MS m/z 216 (MH^+). ^{1}H NMR (DMSO-d_6) δ 1.22 (d, 6H), 2.93 (m, 1H), 7.16 (s, 2H), 7.23 (d, 2H), 7.35 (d, 2H). ^{13}C NMR (DMSO-d_6) δ 23.7, 33.1, 126.6, 126.7, 129.1, 134.5, 148.0, 170.0.

1-(4-Heptylphenyl)maleimide (12). White-off crystalline solid. Yield: 74%. Mp 55−56 °C. GC−MS m/z 272 (MH^+). ^{1}H NMR (DMSO-d_6) δ 0.86 (t, 3H), 1.28 (d, 8H), 1.58 (t, 2H), 2.60 (t, 2H), 7.16 (d, 2H), 7.21 (d, 2H), 7.29 (d, 2H). ^{13}C NMR ($CDCl_3$) δ 13.8, 22.0, 28.4, 28.5, 30.8, 31.2, 34.6, 126.6, 128.6, 129.0, 134.6, 142.0, 170.0.

1-(4-Hydroxyphenyl)maleimide (13). Golden crystalline solid. Yield: 87%. Mp 188−190 °C. GC−MS m/z 190 (MH^+). ^{1}H NMR (DMSO-d_6) δ 2.29 (s, 2H), 7.19 (s, 2H), 7.25 (m, 2H), 7.38 (m, 2H). ^{13}C NMR (DMSO-d_6) δ 122.3, 127.9, 134.6, 149.5, 169.8.

1-(2-Methoxyphenyl)maleimide (14). Brown crystalline solid. Yield: 88%. Mp 109−111 °C. GC−MS m/z 204 (MH^+). ^{1}H NMR ($CDCl_3$) δ 6.82 (s, 2H), 7.02 (q, 2H), 7.16 (d, 1H), 7.39 (t, 1H), 3.78 (s, 3H). ^{13}C NMR ($CDCl_3$) δ 55.8, 112.1, 119.8, 130.0, 134.5, 155.4, 169.7.

1-(3-Methoxyphenyl)maleimide (15). Yellow crystalline solid. Yield: 76%. Mp 68−70 °C. GC−MS m/z 204 (MH^+). ^{1}H NMR (DMSO-d_6) δ 3.77 (s, 3H), 6.91 (m, 2H), 6.98 (d, 1H), 7.17 (s, 2H), 7.38 (t, 1H). ^{13}C NMR (DMSO-d_6) δ 55.9, 112.7, 113.2, 118.9, 129.5, 132.5, 134.5, 159.3, 170.0.

1-(4-Methoxyphenyl)maleimide (16). Green crystalline solid. Yield: 84%. Mp 136−138 °C. GC−MS m/z 204 (MH^+). ^{1}H NMR ($CDCl_3$) δ 3.81 (s, 3H), 6.81 (s, 2H), 6.97 (s, 2H), 7.22 (d, 2H). ^{13}C NMR ($CDCl_3$) δ 55.5, 114.5, 123.9, 127.6, 134.1, 159.2, 169.8.

1-(2-Fluorophenyl)maleimide (17). Pale-yellow crystalline solid. Yield: 62%. Mp 74−75 °C. GC−MS m/z 192 (MH^+). ^{1}H NMR (DMSO-d_6) δ 7.50−7.56 (m, 1H), 7.40−7.47 (m, 2H), 7.35 (t, 1H), 7.27 (s, 2H). ^{13}C NMR ($CDCl_3$) δ 116.7, 116.9, 124.7, 129.8, 130.7, 130.8, 134.7, 168.7.

1-(3-Fluorophenyl)maleimide (18). Yellow crystalline solid. Yield: 48%. Mp 61−62 °C. GC−MS m/z 192 (MH^+). ^{1}H NMR (DMSO-d_6) δ 7.20 (s, 2H), 7.32 (d, 2H), 7.70 (d, 2H). ^{13}C NMR ($CDCl_3$) δ 125.9, 128.0, 128.4, 133.9, 141.1, 169.3.

1-(4-Fluorophenyl)maleimide (19). Yellow crystalline solid. Yield: 72%. Mp 146−148 °C. GC−MS m/z 192 (MH^+). ^{1}H NMR ($CDCl_3$) δ 6.83 (s, 2H), 7.14 (t, 2H), 7.32(q, 2H). ^{13}C NMR ($CDCl_3$) δ 116.0, 127.2, 127.9, 134.2, 160.6, 169.4.

1-(2-Chlorophenyl)maleimide (20). Orange crystalline solid. Yield: 86%. Mp 74−75 °C. GC−MS m/z 208 (MH^+). ^{1}H NMR ($CDCl_3$) δ 6.88 (s, 2H), 7.26 (d, 1H), 7.37 (m, 2H), 7.53 (d, 2H). ^{13}C NMR ($CDCl_3$) δ 127.6, 129.0, 130.3, 130.6, 133.1, 134.4, 168.7.

1-(3-Chlorophenyl)maleimide (21). Yellow crystalline solid. Yield: 77%. Mp 66−69 °C. GC−MS m/z 208 (MH^+). ^{1}H NMR ($CDCl_3$) δ 6.84 (s, 2H), 7.28 (d, 1H), 7.34 (d, 2H), 7.38 (d, 1H), 7.40 (t, 1H). ^{13}C NMR ($CDCl_3$) δ 124.0, 126.1, 128.1, 130.1, 132.4, 134.3, 135.7, 169.0.

1-(4-Chlorophenyl)maleimide (22). Yellow crystalline solid. Yield: 94%. Mp 114−115 °C. GC−MS m/z 208 (MH^+). ^{1}H NMR ($CDCl_3$) δ 6.84 (s, 2H), 7.25 (d, 2H), 7.58 (d, 2H). ^{13}C NMR ($CDCl_3$) δ 119.4, 125.2, 128.2, 130.2, 132.2, 170.0.

1-(2-Bromophenyl)maleimide (23). Pale-white crystalline solid. Yield: 76%. Mp 78−80 °C. GC−MS m/z 253 (MH^+). ^{1}H NMR ($CDCl_3$) δ 6.86 (s, 2H), 7.25 (d, 1H), 7.31 (t, 1H), 7.42 (t, 1H), 7.70 (d, 1H). ^{13}C NMR ($CDCl_3$) δ 122.3, 128.4, 130.8, 133.6, 134.5, 168.8.

1-(3-Bromophenyl)maleimide (24). Golden needles. Yield: 78%. Mp 114−116 °C. GC−MS m/z 253 (MH^+). ^{1}H NMR ($CDCl_3$) δ 7.26 (s, 2H), 7.34 (d, 2H), 7.51 (m, 1H), 7.56 (s, 1H). ^{13}C NMR ($CDCl_3$) δ 124.5, 128.9, 130.3, 130.9, 132.5, 134.3, 135.2, 169.0.

1-(4-Bromophenyl)maleimide (25). Yellow crystalline solid. Yield: 87%. Mp 128−130 °C. GC−MS m/z 253 (MH^+). ^{1}H NMR ($CDCl_3$) δ 1.32- 1.41 (m, 4H), 1.59−1.62 (m, 2H), 1.68−1.71 (m, 2H), 2.58 (t, 2H), 3.04 (t, 2H), 7.09−7.14 (m, 3H), 7.19−7.22 (m, 2H), 7.62 (s, 1H). ^{13}C NMR ($CDCl_3$) δ 121.5, 127.4, 130.3, 132.2, 134.3, 169.1.

1-(2-Iodophenyl)maleimide (26). Brown needles. Yield: 88%. Mp 102−104 °C. GC−MS m/z 300 (MH^+). ^{1}H NMR ($CDCl_3$)

δ 7.25 (s, 2H), 7.42 (d, 1H), 7.53 (t, 1H), 7.99 (d, 1H). ^{13}C NMR ($CDCl_3$) δ 98.9, 129.4, 130.3, 131.0, 134.5, 139.8, 168.7.

1-(3-Iodophenyl)maleimide (27). Yellow crystalline solid. Yield: 72%. Mp 154−155 °C. GC−MS *m*/*z* 300 (MH^+). ^{1}H NMR (DMSO-d_6) δ 7.19 (s, 2H), 7.29 (t, 1H), 7.39 (t, 1H), 7.77 (d, 2H). ^{13}C NMR ($CDCl_3$) δ 93.9, 126.1, 130.7, 132.8, 134.7, 134.9, 136.2, 169.5.

1-(4-Iodophenyl)maleimide (28). Yellow crystalline solid. Yield: 90%. Mp 145−147 °C. GC−MS *m*/*z* 300 (MH^+). ^{1}H NMR ($CDCl_3$) δ 6.85 (s, 2H), 7.13 (d, 2H), 7.79 (d, 2H). ^{13}C NMR ($CDCl_3$) δ 127.6, 131.1, 134.3, 138.3, 169.0.

1-Biphenyl-2-ylmaleimide (29). White crystalline solid. Yield: 84%. Mp 138−140 °C. GC−MS *m*/*z* 250 (MH^+). ^{1}H NMR (DMSO-d_6) δ 7.05 (s, 2H), 7.14 (d, 2H), 7.31−7.41 (m, 4H), 7.47−7.57 (m, 4H). ^{13}C NMR (DMSO-d_6) δ 126.4, 126.5, 127.3, 127.8, 128.4, 128.9, 129.2, 133.6, 137.2, 139.8, 168.8.

1-Biphenyl-3-ylmaleimide (30). Yellow crystalline solid. Yield: 61%. Mp 76−78 °C. GC−MS *m*/*z* 250 (MH^+). ^{1}H NMR ($CDCl_3$) δ 6.87 (s, 2H), 7.31−7.36 (m, 2H), 7.44 (t, 3H), 7.51−7.60 (m, 5H). ^{13}C NMR ($CDCl_3$) δ 122.7, 122.9, 125.2, 124.7, 125.7, 126.8, 127.4, 129.6, 132.2, 138.1, 140.4, 167.4.

1-Biphenyl-4-ylmaleimide (31). Yellow crystalline solid. Yield: 97%. Mp 176−178 °C. GC−MS *m*/*z* 250 (MH^+). ^{1}H NMR (DMSO-d_6) δ 6.88 (s, 2H), 7.37 (t, 1H), 7.42−7.47 (m, 4H), 7.59 (d, 2H), 7.68 (d, 2H). ^{13}C NMR (DMSO-d_6) δ.13.8, 22.0, 26.0, 27.8, 31.2, 37.0, 134.4, 171.0.

1-Benzylmaleimide (32). Beige crystalline solid. Yield: 67%. Mp 68−71 °C. GC−MS *m*/*z* 188 (MH^+). ^{1}H NMR (DMSO-d_6) δ 4.60 (s, 2H), 7.08 (s, 2H), 7.24−7.33 (m, 6H). ^{13}C NMR ($CDCl_3$) δ 41.5, 120.1, 127.9, 127.4, 128.7, 134.3, 136.2, 170.4.

1-Phenethylmaleimide (33). Beige crystalline solid. Yield: 76%. Mp 109−112 °C. GC−MS *m*/*z* 202 (MH^+). ^{1}H NMR (DMSO-d_6) δ 1.06 (t, 2H), 2.82 (t, 2H), 6.97 (s, 2H), 7.15 (d, 2H), 7.20 (d, 1H), 7.27 (t, 2H). ^{13}C NMR (DMSO-d_6) δ 33.5, 38.3, 126.3, 128.2, 128.5, 134.3, 138.0, 170.6.

1-(4-Phenylbutyl)maleimide (34). White crystalline solid. Yield: 68%. Mp 60−62 °C. GC−MS *m*/*z* 230 (MH^+). ^{1}H NMR ($CDCl_3$) δ 1.67−1.57 (m, 4H), 2.64 (d, 2H), 3.54 (t, 2H), 6.67 (s, 2H), 7.16 (d, 3H), 7.30−7.24 (m, 3H). ^{13}C NMR ($CDCl_3$) δ 28.1, 28.5, 35.3, 37.3, 125.9, 128.4, 134.1, 142.0, 170.9.

1-(4-Ethylbenzyl)maleimide (35). White-yellow powder. Yield: 96%. Mp 47−48 °C. GC−MS *m*/*z* 216 (MH^+). ^{1}H NMR (DMSO-d_6) δ 1.14 (m, 3H), 2.56 (m, 2H), 4.55 (s, 2H), 7.06 (s, 2H), 7.15 (m, 4H). ^{13}C NMR (DMSO-d_6) δ 15.5, 27.7, 40.2, 127.2, 127.8, 133.9, 134.6, 142.9, 170.7.

***N*-Phenylsuccinimide (37). 37** was synthesized similarly to **1** using succinic anhydride instead of maleic anhydride. White crystalline solid. Yield: 89%. Mp 154−157 °C. GC−MS *m*/*z* 176 (MH^+). ^{1}H NMR (DMSO-d_6) δ 2.54 (q, 4H), 7.01 (t, 1H), 7.28 (t, 2H), 7.58 (d, 2H). ^{13}C NMR (DMSO-d_6) δ 28.7, 30.9, 118.8, 122.8, 128.6, 139.2, 170.0, 173.7.

***N*-Phenylphtalimide (38). 38** was synthesized similarly to **1** using phthalic anhydride instead of maleic anhydride. White crystalline solid. Yield: 84%. Mp 201−203 °C. GC−MS *m*/*z* 224 (MH^+). ^{1}H NMR ($CDCl_3$) δ 7.42 (m, 3H), 7.51 (t, 2H), 7.79 (d, 2H), 7.96 (d, 2H). ^{13}C NMR ($CDCl_3$) δ 123.8, 126.6, 128.1, 129.1, 131.7, 131.8, 134.4, 167.3.

3-Methyl-1-phenylmaleimide (39). 39 was obtained as **1** using methylmaleic anhydride instead of maleic anhydride. White solid recrystallized from ethanol. Yield: 37%. Mp 98−100 °C. GC−MS *m*/*z* 188 (MH^+). ^{1}H NMR (DMSO-d_6) δ 2.06 (s, 3H), 6.05 (s, 1H), 7.04 (d, 1H), 7.28 (d, 2H), 7.60 (q, 2H). ^{13}C NMR (DMSO-d_6) δ 21.6, 119.3, 121.1, 123.0, 123.2, 128.6, 139.3, 146.9, 168.2.

3,4-Dimethyl-1-phenylmaleimide (40). 40 was obtained as **1** using dimethylmaleic anhydride instead of maleic anhydride. White crystalline solid recrystallized from ethanol. Yield: 40%. Mp 78−79 °C. GC−MS *m*/*z* 202 (MH^+). ^{1}H NMR (DMSO-d_6) 2.03 (s, 3H), 7.02 (t, 1H), 7.28 (t, 2H), 7.56 (d, 2H). ^{13}C NMR (DMSO-d_6) δ 9.1, 118.8, 122.8, 128.5, 139.2, 140.3, 166.4.

1,3-Diphenylmaleimide (41). 41 was obtained as **1** using phenylmaleic anhydride instead of maleic anhydride. White crystalline solid recrystallized from ethanol. Yield: 51%. Mp 116−117 °C. GC−MS *m*/*z* 250 (MH^+). ^{1}H NMR (DMSO-d_6) δ 7.27 (s, 1H), 7.47 (m, 4H), 7.55 (m, 2H), 7.67 (m, 4H). ^{13}C NMR (DMSO-d_6) δ 126.5, 126.6, 129.8, 129.9, 130.0, 130.1, 130.2, 168.4.

General Procedure for the Preparation of *N*-Alkylmaleimide (Method B) (Mitsunobu Coupling) (36, 44−46). A 250 mL round-bottom flask was charged with PPh_3 (2.70 g, 10.3 mmol) to which was added 70 mL of anhydrous THF. The resulting clear solution was cooled to −78 °C. Diethylazodicarboxylate (1.63 mL, 10.3 mmol) was added over a period of 2−3 min. The yellow reaction mixture was stirred during 5 min, after which the desired alcohol (11.3 mmol) was added over 1 min and stirred for 5 min. Neopentyl alcohol (0.50 g, 5.7 mmol) and maleimide (1.00 g, 10.3 mmol) were added sequentially to the reaction mixture as solids. The resulting suspension was allowed to remain at −78 °C for 5 min during which time most of the maleimide dissolved. The cooling bath was then removed, and the mixture was stirred overnight at room temperature. The clear solution was evaporated under reduced pressure and the resulting solid recrystallized from ethanol or purified by column chromatography.

1-Biphenyl-4-ylmethylmaleimide (36). 36 was synthesized starting from 4-biphenylmethanol. Yellow crystalline solid recrystallized from ethanol. Yield: 96%. Mp 155−159 °C. GC−MS *m*/*z* 264 (MH^+). ^{1}H NMR ($CDCl_3$) δ 7.54 (d, 4H), 7.42 (t, 4H), 7.34 (t, 1H), 6.72 (s, 2H), 4.72 (s, 2H). ^{13}C NMR ($CDCl_3$) δ 41.2, 127.1, 127.4, 127.5, 128.8, 128.9, 134.3, 135.2, 140.7, 170.4.

***N*-Nonylmaleimide (44). 44** was synthesized starting from 1-nonanol. White solid purified by column chromatography (silica) using dichloromethane as eluent. Yield: 65%. Mp 46−49 °C. GC−MS *m*/*z* 224 (MH^+). ^{1}H NMR (DMSO-d_6) δ 0.85 (t, 3H), 1.23 (m, 12H), 1.45 (m, 2H), 3.38 (t, 2H), 7.00 (s, 2H). ^{13}C NMR (DMSO-d_6) δ 13.9, 22.0, 27.8, 31.5, 54.8, 134.3, 134.7, 171.0.

***N*-Palmitylmaleimide (45). 45** was synthesized starting from 1-hexadecanol. White solid recrystallized from ethanol. Yield: 93%. Mp 67−68 °C. GC−MS *m*/*z* 322 (MH^+). ^{1}H NMR ($CDCl_3$) δ 0.88 (t, 3H), 1.25 (m, 26H), 1.57 (t, 2H), 3.50 (t, 2H), 6.98 (s, 2H). ^{13}C NMR ($CDCl_3$) δ 14.1, 22.7, 26.8, 28.6, 29.2, 29.4, 29.5, 29.6, 29.7, 32.0, 38.0, 134.1, 171.0.

***N*-Oleylmaleimide (46). 46** was synthesized starting from oleyl alcohol. White solid. Purified by column chromatography (silica) using dichloromethane as eluent. Yield: 48%. Mp < 20 °C. GC−MS *m*/*z* 348 (MH^+). ^{1}H NMR (DMSO-d_6) δ 0.85 (t, 3H), 1.23 (m, 18H), 1.47 (t, 2H), 1.97 (m, 4H), 3.37 (t, 2H), 5.32 (t, 2H), 7.00 (s, 2H). ^{13}C NMR (DMSO-d_6) δ 13.8, 22.0, 26.0, 27.8, 28.4, 28.5, 28.6, 28.7, 29.0, 31.2, 36.9, 129.5, 134.3, 171.0.

Procedure for the Preparation of the 1,4-Bis(malimido)xylene (49). This procedure is similar to the procedure for **2**. However, 2 equiv of the appropriate amine are used (40 mmol) instead of 1.

1,4-Bis(malimido)xylene (49). Beige solid. Recrystallized from ethanol. Yield: 46%. Mp > 250 °C. GC−MS *m*/*z* 297 (MH^+). ^{1}H NMR ($CDCl_3$) δ 4.56 (s, 4H), 7.06 (s, 4H), 7.18 (s, 4H). ^{13}C NMR (DMSO-d_6) δ 40.0, 127.4, 134.6, 135.8, 170.7.

Pharmacological Assays. MGL Activity Assay. Measurement of radiolabeled 2-oleoylglycerol (2-OG) hydrolysis was performed as previously described.[35] Briefly, 2-OG (10 μM, [^{3}H]-2-OG 50,000 dpm, American Radiolabeled Chemicals, in Tris buffer, pH 8.0, 50 mM with 0.6% BSA) was incubated at 37 °C for 10 min in the presence of purified recombinant human MGL[26] (5 ng in 50 mM Tris buffer, pH 8.0, 0.1% BSA, 200 μL of total volume assay) and either dimethyl sulfoxide (controls) or tested compounds. The incubation was stopped by adding 400 μL of an ice-cold 1:1 methanol−chloroform mixture to each tube and thorough mixing. After centrifugation at 700*g* for 5 min, radioactivity in the upper aqueous layer was measured

by liquid scintillation. Blanks (i.e., tubes containing no enzyme) were made for each experiment (and the values subtracted from all the other values).

FAAH Activity Assay. Briefly,[36] FAAH (in 165 μL of Tris-HCl, pH 7.4) was added on ice to glass tubes containing either tested compounds or dimethyl sulfoxide (10 μL). Hydrolysis was initiated by adding 25 μL of [^{3}H]anandamide (50 000 dpm, American Radiolabeled Chemicals, 2 μM final concentration) in Tris-HCl containing 0.1% BSA, and tubes were incubated for 10 min at 37 °C. Reactions were stopped by rapidly placing the tubes on ice and adding 400 μL of ice-cold methanol−chloroform (1:1 v/v). Following centrifugation (850*g*, 5 min, 4 °C) the [^{3}H]ethanolamine in the aqueous layer was recovered (200 μL) and counted by liquid scintillation. Blanks were prepared (buffer instead of FAAH) and the values systematically subtracted.

MGL Preincubation Assay. Purified recombinant human MGL (5 ng in 50 mM Tris buffer, pH 8.0, 0.1% BSA, 200 μL of total volume assay) was preincubated for 0, 15, or 30 min with 10 μL of ATFMK (6.3 μM), *N*-phenylmaleimide (**2**, 16 μM), or bismalemidoxylyl (**49**, 2 μM) at room temperature. Then, 25 μL of 2-OG (10 μM final concentration, [^{3}H]-2-OG 50,000 dpm, American Radiolabeled Chemicals, in Tris buffer, pH 8.0, 50 mM with 0.6% BSA) was added and the resulting preparation incubated at 37 °C for 10 min. The incubation was stopped by adding 400 μL of an ice-cold 1:1 methanol−chloroform mixture to each tube and thorough mixing. After centrifugation at 700*g* for 5 min, radioactivity in the upper aqueous layer was measured by liquid scintillation. Blanks (i.e., tubes containing no enzyme) were made for each experiment (and the values subtracted from all the other values).

MGL Irreversible Inhibition Assay. The assay was performed as previously reported.[20] Briefly, an amount of 2.5 μL of an inhibitor solution in dimethyl sulfoxide at 40 times its IC_{50} value (except for MAFP, at 20 times its IC_{50} value) was added to 50 μL of assay buffer (Tris buffer, pH 8.0, 50 mM, 0.05% BSA) containing 0.22 μg of MGL and incubated at room temperature for 1 h. Two aliquots of 5 μL of the solution were then taken, and each was added to 1495 μL of assay buffer. An amount of 150 μL of the resulting solution was then added to a test tube containing 10 μL of dimethyl sulfoxide (in duplicates). An amount of 40 μL of 2-OG (10 mM, [^{3}H]-2-OG 50,000 dpm, American Radiolabeled Chemicals, in Tris buffer, pH 8.0, 50 mM with 0.6% BSA) was added and the solution incubated for 10 min at 37 °C. The incubation was stopped by adding 400 μL of an ice-cold 1:1 methanol−chloroform mixture to each tube and thorough mixing. After centrifugation at 1700*g* for 5 min, radioactivity in the upper aqueous layer was measured by liquid scintillation. Controls (i.e., tubes containing 2.5 μL of dimethyl sulfoxide instead of the inhibitor solution) and blanks (i.e., tubes containing 2.5 μL of dimethyl sulfoxide instead of the inhibitor solution and 150 μL of buffer instead of the solution C) were made for each experiment (and the value for blanks systematically subtracted).

Acknowledgment. The authors thank Dr. S. Saario for the gift of NAM, used for the preliminary experiments. The help of Professor G. K. E. Scriba of University of Iena, Germany, and of Dr. G. Chataigné, UCL, with the mass spectra and elemental analysis is gratefully acknowledged. This study was supported by grants from the Belgian National Fund for Scientific Research (FRFC No. 2.4.654.06 F) and FSR grants from the Université Catholique de Louvain.

Supporting Information Available: Characteristic infrared peaks of compounds **3**−**46** and **49** and elemental analysis data of compounds **12** and **35**. This material is available free of charge via the Internet at http://pubs.acs.org.

References

(1) Saario, S. M.; Salo, O. M.; Nevalainen, T.; Poso, A.; Laitinen, J. T.; Jarvinen, T.; Niemi, R. Characterization of the Sulfhydryl-Sensitive Site in the Enzyme Responsible for Hydrolysis of 2-Arachidonoylglycerol in Rat Cerebellar Membranes. *Chem. Biol.* **2005**, *12*, 649–656.
(2) Lambert, D. M.; Fowler, C. J. The Endocannabinoid System: Drug Targets, Lead Compounds, and Potential Therapeutic Applications. *J. Med. Chem.* **2005**, *48*, 5059–5087.
(3) Cravatt, B. F.; Giang, D. K.; Mayfield, S. P.; Boger, D. L.; Lerner, R.; Gilula, N. B. Molecular Characterization of an Enzyme that Degrades Neuromodulatory Fatty Acid Amides. *Nature* **1996**, *384*, 83–87.
(4) Karlsson, M.; Contreras, J. A.; Hellman, U.; Tornqvist, H.; Holm, C. cDNA Cloning, Tissue Distribution, and Identification of the Catalytic Triad of Monoglyceride Lipase. Evolutionary Relationship to Esterases, Lysophospholipases, and Haloperoxidases. *J. Biol. Chem.* **1997**, *272*, 27218–27223.
(5) Tornqvist, H.; Belfrage, P. Purification and Some Properties of a Monoacylglycerol-Hydrolyzing Enzyme of Rat Adipose Tissue. *J. Biol. Chem.* **1976**, *251*, 813–819.
(6) Wei, B. Q.; Mikkelsen, T. S.; McKinney, M. K.; Lander, E. S.; Cravatt, B. F. A Second Fatty Acid Amide Hydrolase with Variable Distribution among Placental Mammals. *J. Biol. Chem.* **2006**, *281*, 36569–36578.
(7) Tsuboi, K.; Sun, Y.-X.; Okamoto, Y.; Araki, N.; Tonai, T.; Ueda, N. Molecular Characterization of *N*-Acylethanolamine-Hydrolyzing Acid Amidase, a Novel Member of the Choloylglycine Hydrolase Family with Structural and Functional Similarity to Acid Ceramidase. *J. Biol. Chem.* **2005**, *280*, 11052–11092.
(8) Blankman, J. L.; Simon, G. M.; Cravatt, B. F. A Comprehensive Profile of Brain Enzymes that Hydrolyze the Endocannabinoid 2-Arachidonoylglycerol. *Chem. Biol.* **2007**, *14*, 1347–1356.
(9) Saario, S. M.; Laitinen, J. T. Monoglyceride Lipase as an Enzyme Hydrolyzing 2-Arachidonoylglycerol. *Chem. Biodiversity* **2007**, *4*, 1903–1913.
(10) Mechoulam, R.; Ben-Shabat, S.; Hanus, L.; Ligumsky, M.; Kaminski, N. E.; Schatz, A. R.; Gopher, A.; Almog, S.; Martin, B. R.; Compton, D. R.; Pertwee, R. G.; Griffin, G.; Bayewitch, M.; Barg, J.; Vogel, Z. Identification of an Endogenous 2-Monoglyceride, Present in Canine Gut, That Binds to Cannabinoid Receptors. *Biochem. Pharmacol.* **1995**, *50*, 83–90.
(11) Sugiura, T.; Kondo, S.; Sukagawa, A.; Nakane, S.; Shinoda, A.; Itoh, K.; Yamashita, A.; Waku, K. 2-Arachidonoylglycerol. A Possible Endogenous Cannabinoid Receptor−Ligand in Brain. *Biochem. Biophys. Res. Commun.* **1995**, *215*, 89–97.
(12) Wilson, R. I.; Nicoll, R. A. Endogenous Cannabinoids Mediate Retrograde Signalling at Hippocampal Synapses. *Nature* **2001**, *410*, 588–592.
(13) Gulyas, A. I.; Cravatt, B. F.; Bracey, M. H.; Dinh, T. P.; Piomelli, D.; Boscia, F.; Freund, T. F. Segregation of Two Endocannabinoid-Hydrolyzing Enzymes into Pre- and Postsynaptic Compartments in the Rat Hippocampus, Cerebellum and Amygdala. *Eur. J. Neurosci.* **2004**, *20*, 441–458.
(14) Dinh, T. P.; Carpenter, D.; Leslie, F. M.; Freund, T. F.; Katona, I; Sensi, S. L.; Kathuria, S.; Piomelli, D. Brain Monoglyceride Lipase Participating in Endocannabinoid Inactivation. *Proc. Natl. Acad. Sci. U.S.A.* **2002**, *99*, 10819–10824.Erratum in the following: *Proc. Natl. Acad. Sci. U.S.A.* **2002**, *99* (21), 13961.
(15) Dinh, T. P.; Kathuria, S.; Piomelli, D. RNA Interference Suggests a Primary Role for Monoacylglycerol Lipase in the Degradation of the Endocannabinoid 2-Arachidonoylglycerol. *Mol. Pharmacol.* **2004**, *66*, 1260–1264.
(16) Muccioli, G. G.; Xu, C.; Odah, E.; Cudaback, E.; Cisneros, J. A.; Lambert, D. M.; Lopez Rodriguez, M. L.; Bajjalieh, S.; Stella, N. Identification of a Novel Endocannabinoid-Hydrolyzing Enzyme Expressed by Microglial Cells. *J. Neurosci.* **2007**, *27*, 2883–2889.
(17) Stella, N. Endocannabinoid Signalling in Microglial Cells. *Neuropharmacology* **2009**, *56*, 244–253.
(18) Karlsson, M.; Reue, K.; Xia, Y. R.; Lusis, A. J.; Langin, D.; Tornqvist, H.; Holm, C. Exon-Intron Organization and Chromosomal Localization of the Mouse Monoglyceride Lipase Gene. *Gene* **2001**, *11* (272), 11–18.
(19) Viso, A.; Cisneros, J. A.; Ortega-Gutierrez, S. The Medicinal Chemistry of Agents Targeting Monoacylglycerol Lipase. *Curr. Top. Med. Chem.* **2008**, *8*, 231–246.
(20) Vandevoorde, S. Overview of the Chemical Families of Fatty Acid Amide Hydrolase and Monoacylglycerol Lipase Inhibitors. *Curr. Top. Med. Chem.* **2008**, *8*, 247–267.
(21) Long, J. Z.; Li, W.; Booker, L.; Burston, J. J.; Kinsey, S. G.; Schlosburg, J. E.; Pavon, F. J.; Serrano, A. M.; Selley, D. E.;

Parsons, L. H.; Lichtman, A. H.; Cravatt, B. F. Selective Blockade of 2-Arachidonoylglycerol Hydrolysis Produces Cannabinoid Behavioral Effects. *Nat. Chem. Biol.* **2009**, *5*, 37–44.
(22) Saario, S. M.; Savinainen, J. R.; Laitinen, J. T.; Jarvinen, T.; Niemi, R. Monoglyceride Lipase-like Enzymatic Activity Is Responsible for Hydrolysis of 2-Arachidonoylglycerol in Rat Cerebellar Membranes. *Biochem. Pharmacol.* **2004**, *67*, 1381–1387.
(23) Cava, M. P.; Deana, A. A.; Muth, K.; Mitchell, M. *N*-Phenylmaleimide. *Org. Synth.* **1961**, *41*, 93–95.
(24) Walker, A. M. A High Yielding Synthesis of *N*-Alkylmaleimides Using a Novel Modification of the Mitsunobu Reaction. *J. Org. Chem.* **1995**, 5352–5355.
(25) Muccioli, G. G.; Labar, G.; Lambert, D. M. CAY10499, a Novel Monoglyceride Lipase Inhibitor Evidenced by an Expeditious MGL Assay. *ChemBioChem* **2008**, *9*, 2704–2710.
(26) Labar, G.; Bauvois, C.; Muccioli, G. G.; Wouters, J.; Lambert, D. M. Disulfiram is an Inhibitor of Human Purified Monoacylglycerol Lipase, the Enzyme Regulating 2-Arachidonoylglycerol Signaling. *ChemBioChem* **2007**, *8*, 1293–1297.
(27) Vandevoorde, S; Jonsson, K. O.; Labar, G.; Persson, E.; Lambert, D. M.; Fowler, C. J. Lack of Selectivity of URB602 for 2-Oleoylglycerol Compared to Anandamide Hydrolysis in Vitro. *Br. J. Pharmacol.* **2007**, *150*, 186–191.
(28) Zvonok, N.; Pandarinathan, L.; Williams, J.; Johnston, M.; Karageorgos, I.; Janero, D. R.; Krishnan, S. C.; Makriyannis, A. Covalent Inhibitors of Human Monoacylglycerol Lipase: Ligand-Assisted Characterization of the Catalytic Site by Mass Spectrometry and Mutational Analysis. *Chem. Biol.* **2008**, *15*, 854–862.
(29) Zvonok, N.; Williams, J.; Johnston, M.; Pandarinathan, L.; Janero, D. R.; Li, J.; Krishnan, S. C.; Makriyannis, A. Full Mass Spectrometric Characterization of Human Monoacylglycerol Lipase Generated by Large-Scale Expression and Single-Step Purification. *J. Proteome Res.* **2008**, *7*, 2158–2164.
(30) Burston, J. J.; Sim-Selley, L. J.; Harloe, J. P.; Mahadevan, A.; Razdan, R. K.; Selley, D. E.; Wiley, J. L. *N*-Arachidonyl Maleimide (NAM) Potentiates the Pharmacological and Biochemical Effects of the Endocannabinoid 2-Arachidonylglycerol through Inhibition of Monoacylglycerol Lipase. *J. Pharmacol. Exp. Ther.* **2008**, *327*, 546–553.
(31) Magrioti, V.; Naxakis, G.; Hadjipavlou-Litina, D.; Makriyannis, A.; Kokotos, G. A Novel Monoacylglycerol Lipase Inhibitor with Analgesic and Anti-Inflammatory Activity. *Bioorg. Med. Chem. Lett.* **2008**, *18*, 5424–5427.
(32) Hohmann, A. G.; Suplita, R. L.; Bolton, N. M.; Neely, M. H.; Fegley, D.; Mangieri, R.; Krey, J. F.; Walker, J. M.; Holmes, P. V.; Crystal, J. D.; Duranti, A.; Tontini, A.; Mor, M.; Tarzia, G.; Piomelli, D. An Endocannabinoid Mechanism for Stress-Induced Analgesia. *Nature* **2005**, *435*, 1108–1112.
(33) Comelli, F.; Giagnoni, G.; Bettoni, I.; Colleoni, M.; Costa, B. The Inhibition of Monoacylglycerol Lipase by URB602 Showed an Anti-Inflammatory and Anti-Nociceptive Effect in a Murine Model of Acute Inflammation. *Br. J. Pharmacol.* **2007**, *152*, 787–794.
(34) Bisogno, T.; Ortar, G.; Petrosino, S.; Morera, E.; Palazzo, E.; Nalli, M.; Maione, S.; Di Marzo, V. Development of a Potent Inhibitor of 2-Arachidonoylglycerol Hydrolysis with Antinociceptive Activity in vivo. *Biochim. Biophys. Acta, Mol. Cell Biol. Lipids* **2009**, *1791*, 53–60.
(35) Vandevoorde, S.; Saha, B.; Mahadevan, A.; Razdan, R. K.; Pertwee, R. G.; Martin, B. R.; Fowler, C. J. Influence of the Degree of Unsaturation of the Acyl Side Chain upon the Interaction of Analogues of 1-Arachidonoylglycerol with Monoacylglycerol Lipase and Fatty Acid Amide Hydrolase. *Biochem. Biophys. Res. Commun.* **2005**, *337*, 104–109.
(36) Labar, G.; Vliet, F. V.; Wouters, J.; Lambert, D. M. A MBP-FAAH Fusion Protein as a Tool To Produce Human and Rat Fatty Acid Amide Hydrolase: Expression and Pharmacological Comparison. *Amino Acids* **2008**, *34*, 127–133.